Polym. Bull.
DOI 10.1007/s00289-015-1581-3

ORIGINAL PAPER

Impact on gene expression in response to silver-decorated titania nanomatrix using an in vitro satellite cell culture model

Touseef Amna[1,2] · M. Shamshi Hassan[2,4] · Salem S. Al-Deyab[3] · Myung-Seob Khil[4] · Inho Hwang[1]

Received: 7 May 2015 / Revised: 13 November 2015 / Accepted: 24 November 2015

Abstract Herein we report the synthesis of novel silver-ornamented titanium dioxide crossbreed nanofibers via electrospinning with improved cellular response for possible muscle tissue engineering applications. Titanium isopropoxide and silver nitrate served as precursors to get high aspect ratio silver-decorated titania nanofibers. For a model application in muscle tissue engineering, muscle satellite cells of local Korean Hanwoo were cultured on synthesized hybrid nanofibers. The standard microarray technique has been employed to screen the potential effects of synthesized nanofibers on genome after the culture of cells on hybrid nanofibers. EDX, EPMA, FT-IR, XRD and TEM analysis confirmed purity, distribution, interaction and crystalline nature of this material while the diameter of these nanofibers estimated from FE-SEM and TEM were between 200 and 300 nm. Cell counting with Kit-8 assay at regular time intervals and phase contrast microscopy data revealed that satellite cells proliferated well on nanofibers and cellular attachments were visible by SEM. Microarray analyses of gene expression response indicated clear changes in gene expression in a range of proliferation and apoptosis. Our results open-up new ways to develop and analyze gene expression biomarkers for satellite cell proliferation and finally muscle tissue engineering.

✉ Touseef Amna
touseefamna@gmail.com

✉ Inho Hwang
inho.hwang@jbnu.ac.kr

[1] Department of Animal Science and Biotechnology, Chonbuk National University, Jeonju 561-756, Republic of Korea

[2] Faculty of Science, Albaha University, Albaha 1988, Saudi Arabia

[3] Department of Chemistry, College of Science, King Saud University, Riyadh 11451, Saudi Arabia

[4] Department of Organic Materials and Fiber Engineering, Chonbuk National University, Jeonju 561-756, Republic of Korea

Published online: 11 December 2015

Keywords Tissue engineering · Microarray · Satellite cells · Electrospinning · Hanwoo muscle

Introduction

Ultrafine fiber scaffolds prepared by electrospinning (e-spinning) of a polymer solution have been extensively studied because of their unique property such as high surface area-to-volume ratio. Incorporation of silver nanoparticles into ultrafine fibers has attracted a great deal of attention because the resulting fibers possess strong antimicrobial action. Nanocrystalline silver has been proven to be the most effective antimicrobial agent [1, 2] as silver, and its compounds have powerful antimicrobial activity [2] and broad inhibitory/or biocidal spectra for diverse microbes (for instance bacteria, viruses, and eukaryotic microorganisms) [3–5]. Due to their unique antimicrobial properties; silver nanocrystallites have earned substantial attention and are used extensively for biomedical applications (such as an additive to wound dressings, surgical instruments and bone substitute materials). Silver nanocrystallites are of particular interest because of their well-known bactericidal and fungicidal properties and are widely used in medical devices, textiles, food packaging, and healthcare and household products [6–9]. Moreover, silver sulfadiazine is used clinically to reduce burn or wound infections caused by multidrug resistant bacteria and fungi [10, 11]. Additionally, the silver nanoparticles are also used in the purification of water and air quality management. Similarly, nanostructured titanium dioxide (TiO_2) has also generated great interest due to their high surface to volume ratio and the ability to provoke a greater degree of biological plasticity compared to conventional microstructures [12, 13]. Nanostructured TiO_2 has been widely used in various applications such as biosensors [14] and biomaterials [15, 16]. It is also gaining prominence as an implant material due to its unique properties such as high specific surface area and the ability to exhibit positive cellular response. The influence of TiO_2 nanotubes on cellular response has been investigated using a variety of cell types including osteoblasts [17], fibroblasts [18], chondrocytes [19], endothelial cells [20], muscle cells [20], epidermal keratinocytes [18] and mesenchymal stem cells [12, 21, 22]. Titanium is a material often used in hip and dental implants whose superior biocompatibility are due to the thin layer of TiO_2 that is spontaneously formed at the surface of material. Nowadays the materials based on one-dimensional (1D) nanostructures for instance; nanofibers, nanotubes, nanorods, nanowires, nanobelts, etc., have generated considerable interest due to their unique properties such as size effects, surface effects, magnetism and resulting captivating applications in many fields such as biomedical sciences, sensors, photocatalysis, solar cells, nanoresonators and so on [23]. It has been previously shown that TiO_2 nanotubes can improve osteoblast attachment, function and proliferation [24]. Furthermore, these surfaces also exhibit very low immunogenicity, eliciting low levels of monocyte activation and cytokine secretion [25]. The present study was aimed to evaluate the potential of silver-decorated TiO_2 nanofibers as scaffolds for tissue engineering. So far, a range of

techniques such as template synthesis, phase separation, self-assembly, etc., have been adopted to prepare nanofibers based on polymers, metals, ceramics as well as their composites into two-dimensional (2D) and three-dimensional (3D) nanostructures for diverse practical applications. Nevertheless, the e-spinning is a versatile and superior technique for the fabrication and production of ordered or/more complex nanofibrous architectures/or structures. In addition to traditional 2D nanofibrous structures, e-spinning is powerful in fabrication of 3D fibrous macrostructures, especially for tissue engineering applications [23]. This article condenses the facile e-spinning approach for the fabrication of ID silver-decorated TiO_2 nanofibers and their detailed physico-chemical characterization. The synthesized 1D hybrid nanofibers were utilized for the cultivation of satellite cells with the aim of muscle tissue engineering. For tissue engineering applications, positive cell–scaffold interactions are important. Herein, microarray technique was utilized to identify the expression of specific genes after the interaction of muscle satellite cells with synthesized hybrid matrix. The utilized satellite cells have been isolated from *longissimus dorsi* muscle of native Korean Hanwoo cattle in the present investigation. To the best of our knowledge, there is no report about the cellular response of muscle satellite cells (isolated from *longissimus dorsi*) on the Ag/TiO_2 hybrid nanofibers. Using microarray technique, a total of 290 genes was found to be significantly changed after the cultivation of cells on Ag/TiO_2 hybrid nanofibers. Some genes were up-regulated and some genes were down-regulated in microarray analysis when compared with control muscle cells. Most of the up/down-regulated genes were directly linked-up with cell proliferation, adhesion, migration and growth. On the basis of present results we can conclude that Ag/TiO_2 hybrid nanofibers could be employed in guiding cell adhesion and spreading for muscle growth and regeneration.

Materials and methods

Synthesis and characterization of hybrid nanofibers

The fabrication of Ag-decorated TiO_2 hybrid nanofibers was carried out by facile sol–gel e-spinning process in which titanium isopropoxide and silver nitrate were utilized as precursors for titania and silver, respectively. In brief, titanium isopropoxide (5 mL) was mixed with the alcoholic solution of silver nitrate (10 wt %) solution. Polyvinyl acetate (PVAc, Mw = 500,000 Sigma-Aldrich, USA), pellets were dissolved in *N*,*N*-dimethylformamide (DMF >99.5 assay, Showa Chemicals Ltd., Japan) by continuous stirring ($\sim$8 h) at room temperature to prepare 16 wt % PVAc solution. 6 g of PVAc solution was added gently into the above solution and stirred vigorously. In the present study, PVAc was utilized as the e-spinning carrier. The prepared homogeneous solution was loaded into a plastic syringe (10 ml; equipped with micro-tip) and subsequently placed into an e-spinning setup (ACP Korea Co. Ltd.). A high-voltage power of 20 kV was applied to the needle tip. The nanofibers were collected on a polyethylene sheet wrapped around a ground iron drum placed 18 cm below the needle tip. A copper

pin connected to high-voltage power supply was inserted in the solution as a positive terminal, whereas a ground iron drum served as counter electrode. The e-spinning process was conducted at room temperature. The electrospun Ag–TiO_2 hybrid nanofibers were initially dried at 80 °C for 24 h under vacuum and calcined at 500 °C for 2 h in air. The heating rate was set to be 5 °C/min.

X-ray diffraction (XRD) measurement was carried out using Rigaku/Max-3A X-ray diffractometer equipped with Cu Kα radiation between 10° and 80°. The operating voltage and current were maintained at 30 kV and 40 mA, respectively. Surface morphological images were taken using a field-emission microscope (FE-SEM, JEOL JSM6700, Japan) operated at an accelerating voltage of 5 kV. Energy dispersive X-ray (EDX) measurements were conducted using the EDX system attached to the same microscope, whereas the distribution of elements was measured using electron probe microanalysis (EPMA). To determine the detailed morphological characteristics of the hybrid nanofibers, transmission electron microscopy (TEM) pictures were made using a high-resolution HR-TEM microscope (H-7650, Hitachi, Japan) operated at 200 kV. The infrared (IR) absorption spectroscopy was carried out at room temperature in the range of 400–4000 cm^{-1} by the spectrophotometer (Varian FTS 1000) from the sample prepared as KBr pellets to find out the interaction of Ag and titania.

Hanwoo satellite cell culture

Satellite cells were isolated from *longissimus dorsi* muscle of native Korean Hanwoo according to the previously reported procedure [26]. The entire work involving the use of animals was approved by an Institutional Animal Care and Use Committee and Sacrifices of Animal and was carried out according to International Ethical Committee regulations. Briefly, the *longissimus dorsi* muscle was excised from Hanwoo cattle immediately after slaughter. The epimysium and fat were aseptically trimmed off and discarded. Muscle strips were chopped in a sterilized meat chopper and after enzymatic digestion with pronase (1 mg mL^{-1}) at 37 °C for 60 min; single cells were separated from the tissue fragments by repeated centrifugation. The primary muscle cells were cultured in Dulbecco's modified Eagle's medium (DMEM; Gibco® life technologies, Grand Island, NY, USA) supplemented with 15 % fetal bovine serum (FBS; GIBCO), 100 IU mL^{-1} penicillin, and 100 μg mL^{-1} streptomycin in a humidified incubator at 37 °C with 5 % CO_2. After 80 % confluence, the harvested cells were re-suspended in phosphate-buffered saline (PBS) supplemented with 0.5 % BSA and 2 mM EDTA and centrifuged at 1000×*g* for 10 min. The obtained pellet was re-suspended in PBS (100 μl) containing 10 μg anti-M-cadherin antibodies and then incubated with 20 μL of anti-mouse IgG1 micro beads at 4 °C for 1 h. Finally, the cell suspensions were loaded into a magnetic cell sorting system (AutoMACS, Milteny Biotech, Germany) to isolate satellite cells. The isolated satellite cells were grown in 75 cm^2 culture flask (Bedford, MA, USA) to get the enough cell count. The axenic satellite cells were cultured and maintained in DMEM (pH 7.4) containing 10 % fetal bovine serum and 1 % penicillin–streptomycin solution in a humidified incubator under the same conditions as mentioned above in present study.

In vitro cytotoxicity studies by cell counting kit (CCK)-8 assay

To select a non-cytotoxic concentration range of Ag/TiO_2 hybrid nanofibers to be used for tissue engineering applications; a CCK-8 (Sigma-Aldrich Chemical Co.,USA) viability assay was carried out on isolated satellite cells. The satellite cells were cultured in 96-well plates and then exposed to different concentrations (0–20 μg mL^{-1}) of Ag/TiO_2 nanofibers. The nanofibers were suspended in DMSO and were sonicated to avoid aggregation and then working solutions were made in DMEM. The CCK-8 assay was performed according to manufacturer's instruction to check the cell viability in presence of hybrid nanofibers. After the predetermined culture times, the medium was aspirated and samples were replaced with fresh medium. 10 μL of CCK-8 solution was added into each well and incubated for additional 4 h. After incubation the optical density (OD) was measured at 450 nm in a microplate reader (model 680; Bio-Rad Laboratories, Hercules, CA). The relative cell viability (%) related to control wells was measured using the following equation:

$$\text{Cell viability } (\%) = \text{Abs(test)}/\text{Abs(reference)} \times 100,$$

where Abs(test) is the absorbance of test samples, and Abs(reference) is absorbance of the control sample. Experiments were conducted in replicates and results were expressed as mean [standard deviation (SD) of mean].

Cell morphological examination

Hanwoo muscle cells were seeded at a density of 1×10^5 cells/well in growth medium for 72 h on nanofibrous mat in 6-well plate. The control surfaces were kept without nanofibers. The surfaces were rinsed twice with PBS (1×) and then immobilized as described elsewhere. The surfaces were then subjected to 2–5 min washes with same buffer. The cells were then dehydrated by replacing the buffer with increasing concentrations of ethanol for 10 min each [27]. Finally, the cells were air dried and SEM imaging was conducted as aforementioned in the present study.

Microarray testing

The satellite cells were harvested after 48 h of incubation time to carry out microarray. Both control cells and cells cultivated on nanofibrous matrix were processed using the same method and conditions. Total RNA was extracted from aforementioned cells for microarray analysis. The synthesis of target cRNA probes and hybridization were performed using Agilent's Low Input Quick Amp Labeling Kit (Agilent Technology, USA) strictly following manufacturer's instructions. Briefly, 25 ng total RNA and T7 promoter primer were mixed and incubated at 65 °C for 10 min. cDNA master mix (5× first strand buffer, 0.1 M DTT, 10 mM dNTP mix, RNase-Out, and MMLV-RT) was prepared and added to the reaction mixture. The as-prepared samples were incubated at 40 °C for 2 h. Double strand

DNA (dsDNA) synthesis was terminated by incubating at 70 °C for 10 min. The transcription master mix (4× transcription buffer, 0.1 M DTT, NTP mix, 50 % PEG, RNase-out, inorganic pyrophosphatase, T7-RNA polymerase, and cyanine 3-CTP) was prepared according to manufacturer's protocol. Transcription of dsDNA was performed by adding transcription master mix to dsDNA reaction samples; subsequently incubated at 40 °C for 2 h. The amplified and labeled cRNA was purified on RNase mini column (Qiagen) according to manufacturer's protocol. The labeled CRNA target was quantified using ND-1000 spectrophotometer (NanoDrop Technologies, Inc., Wilmington, DE). After the labeling efficiency check, each 650 ng of cyanine 3-labeled cRNA target was mixed. Additionally, the fragmentation of cRNA was performed by adding 10× blocking agent and 25× fragmentation buffer and incubated at 60 °C for 30 min. The fragmented cRNA was re-suspended with 2× hybridization buffer and directly pipetted onto assembled bovine (V2) gene expression 4 × 44 K microarray (Agilent Technologies). The arrays hybridized at 65 °C for 17 h using an Agilent hybridization oven (Agilent Technology, USA). The hybridized microarrays were washed as per manufacturer's washing protocol (Agilent Technology, USA).

The hybridization images were analyzed by Agilent DNA microarray Scanner (Agilent Technology, USA) and the data quantification was performed using Agilent Feature Extraction software 10.7 (Agilent Technology, USA). The average fluorescence intensity of each spot was calculated and local background was subtracted. All data normalization and selection (fold-change) were performed using GeneSpringGX 7.3.1 (Agilent Technology, USA). Reliable genes were filtered by flag following the Agilent manual. The average of normalized ratio was calculated by dividing the average of control normalized signal intensity by the average of test normalized signal intensity. Functional categorization of gene families over represented was performed using the program from the NIAID web site (http://david.abcc.ncifcrf.gov/summary.jsp).

Results and discussion

E-spinning is a distinctive approach using electrostatic forces to produce ultrafine fibers with diameters in the nanometer to micrometer scale. Basically, an e-spinning system consists of three major components, a high-voltage (kV) power supply with positive or negative polarity, and a syringe with a pipette-tip to carry the solution from the syringe to the grounded collector. The collector is usually a rotating drum that can be covered with aluminum or polyethylene sheet. Although e-spinning is relatively easy to use, many parameters can significantly influence the transformation of polymer solutions into nanofibers. These include the solution properties, working voltage applied at the spinneret tip, spinning distance between the tip and the collector surface, polymer flow-rate and ambient parameters such as solution temperature, humidity, etc. Scheme 1 illustrates the simple setup of e-spinning apparatus used for the fabrication of 1D hybrid nanofibers in the present study.

Figure 1 shows the XRD pattern of Ag/TiO_2 hybrid nanofibers. No distinguish peaks have been detected in the XRD of uncalcined Ag/TiO_2 hybrid nanofibers,

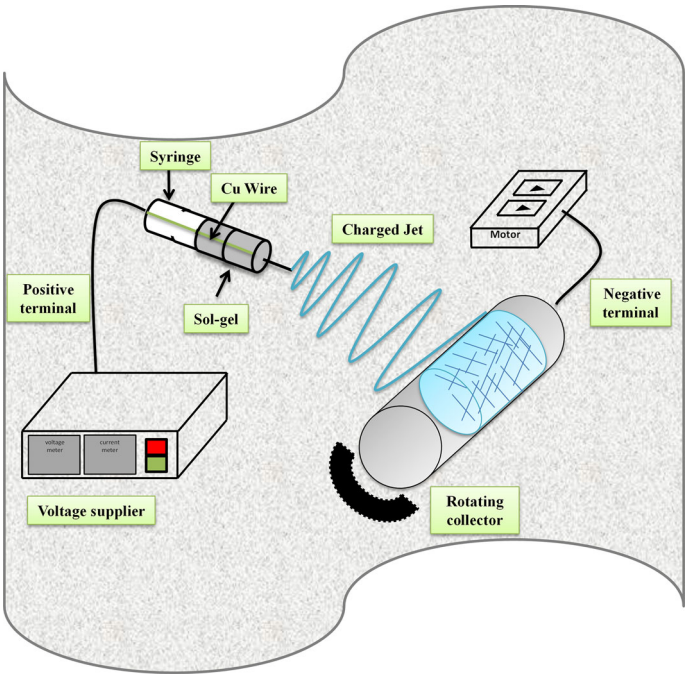

Scheme 1 Schematic diagram of utilized electrospinning setup for the fabrication of silver-decorated titania polymeric hybrid nanofibers for satellite cell culture

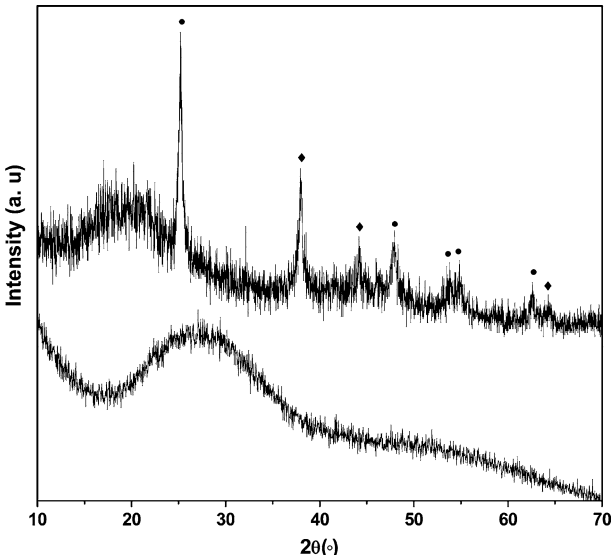

Fig. 1 XRD pattern of the Ag-doped TiO_2 hybrid mat as synthesized and calcined at 500 °C. Symbol (*bullet*) represents TiO_2 and (*diamond*) Ag peaks

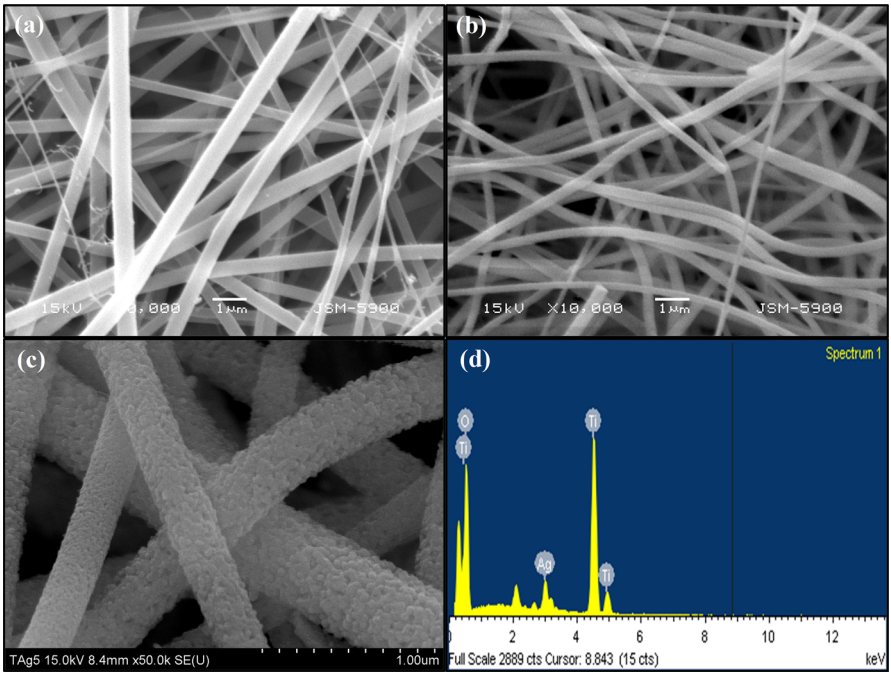

Fig. 2 SEM images of the Ag-doped TiO_2 hybrid mat calcined at 500 °C; **a**, **b** low magnification, **c** high magnification and **d** EDX spectra

whereas after calcination at 500 °C for 2 h, the presence of anatase (A) phase of TiO_2 was clearly observed in the spectra along with Ag (Fig. 1). The peak position at angle 38.1, 44.2 and 64.3 confirms the presence of Ag (JCPDS No. 893722) in the hybrid matrix. Figure 2 demonstrates the FE-SEM images after calcination at 500 °C (Fig. 2a–c). The average diameter of the calcined nanofibers was found to be 350 ± 20 mm. The SEM image of the calcined sample at high resolution demonstrated distinctive nano-sized particle having the porous morphology (Fig. 2c). Figure 2d shows the EDX of the Ag/TiO_2 hybrid nanofibers. Presence of Ag, Ti and O has clearly been observed in the hybrid nanofibers without any impurity. The elemental composition of the hybrid nanofibers was further confirmed by EPMA (Fig. 3). Figure 4a shows the TEM image of Ag/TiO_2 hybrid nanofibers showing densely packed nanocrystals on the surface of nanofibers. The presence of dark color crystals throughout the surface of nanofibers shows the homogeneous distribution of Ag particles in hybrid nanofibers. The SAED pattern composed of bright rings shows the polycrystalline nature of composite nanofibers (inset Fig. 4a). The HR-TEM of the nanofibers (Fig. 4b) revealed the simultaneous presence of the crystalline TiO_2 and Ag crystal lattices in the hybrid nanofibers. The interplaner distance of 0.35 nm was close to the d spacing of the (101) planes of the tetragonal structured TiO_2. The interplaner distances of 0.23 nm agreed well with the lattice spacing of the (111) planes of the cubic structured Ag. This again confirms the presence of Ag particle on TiO_2 surface.

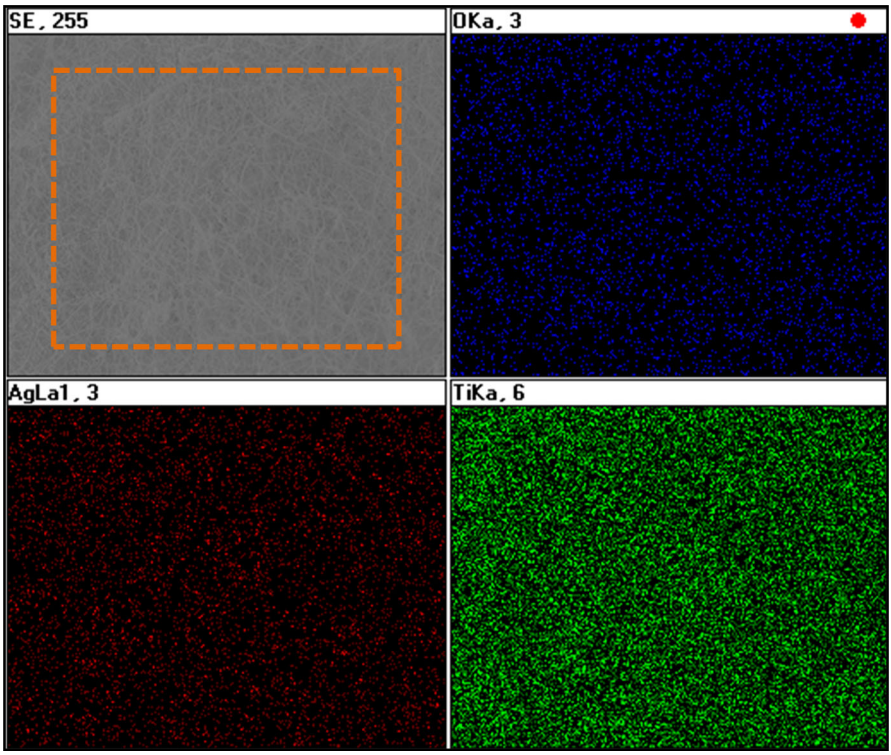

Fig. 3 Electron probe micro-analysis (EPMA) image of Ag-doped TiO_2 hybrid nanofibers

The synthesized Ag/TiO_2 hybrid nanofibers were further analyzed by FT-IR, carried out in the range of 400–4000 cm^{-1} at room temperature (Fig. 5). The large, broad band between 400 and 900 cm^{-1} corresponds to the TiO_2 and Ag ions [28, 29]. The presence of a weak band near 1624 cm^{-1} is assigned to H–O–H bending which may be due to the adsorption of moisture. Bands at 3445 cm^{-1} indicate the presence of OH group. It is evident from the FT-IR data that the Ti–O vibrational mode was more prominently observed, and this clearly concludes a strong doping between Ag and TiO_2 hybrid materials.

To examine the toxic effects of Ag/TiO_2 hybrid nanofibers, satellite cells were incubated with different concentrations (0, 10, 20 μgmL^{-1}) of synthesized nanofibers and viability was determined at regular time intervals. In the present investigation, primary satellite cells were derived directly from adult Korean Hanwoo *longissimus dorsi* muscle. Figure 6 depicts the results of CCK-8 assay. It was observed that growth proceeds in an exponential manner with respect to incubation time. The hybrid nanofibers did not induce reduction of viability. However, the high concentration with extended incubation depicted slight impairment of viability as compared to the control cells. Figure 7a, b shows the microscopic images of unexposed and exposed satellite cells, respectively. More than 80 % confluence was observed in case of control cells and the satellite cells

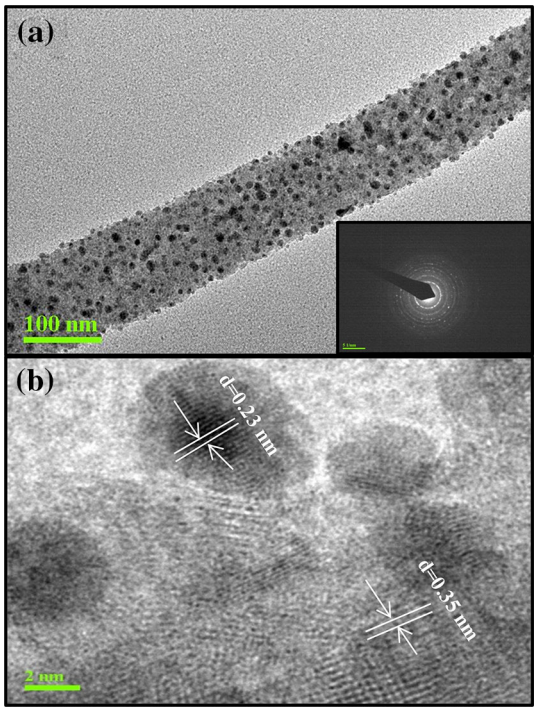

Fig. 4 TEM image of the prepared Ag-doped TiO_2 hybrid at low resolution (**a**) and HR-TEM image (**b**), the SAED pattern (*inset* **a**)

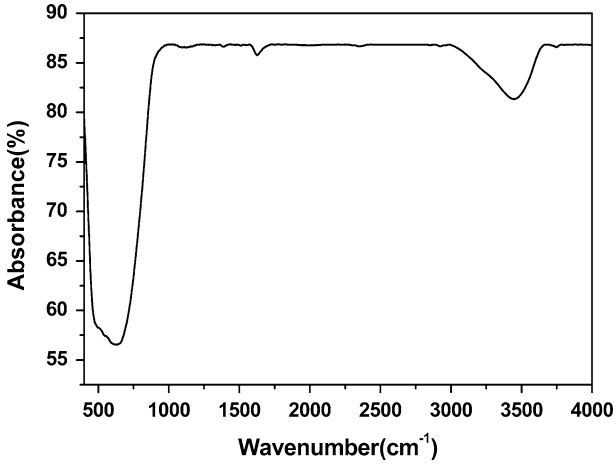

Fig. 5 FT-IR spectra of the prepared Ag-doped TiO_2 hybrid nanofibers

growing on hybrid nanofibers. The living cells have been found to respond differently to materials with nanoscale roughness when compared to smooth surfaces and bulk materials. The viable cells adhere to and spread on the materials by assembling focal adhesions. The focal adhesions are signaling complexes,

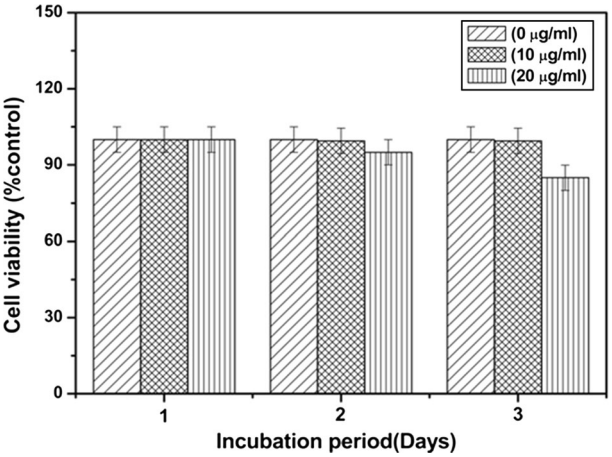

Fig. 6 CCk-8 assay results of satellite cells cultured in the presence of hybrid nanomatrix, the viability of control cells were set 100 %, and viability relative to the control was expressed at different incubation period. The experiments were conducted at least in triplicates

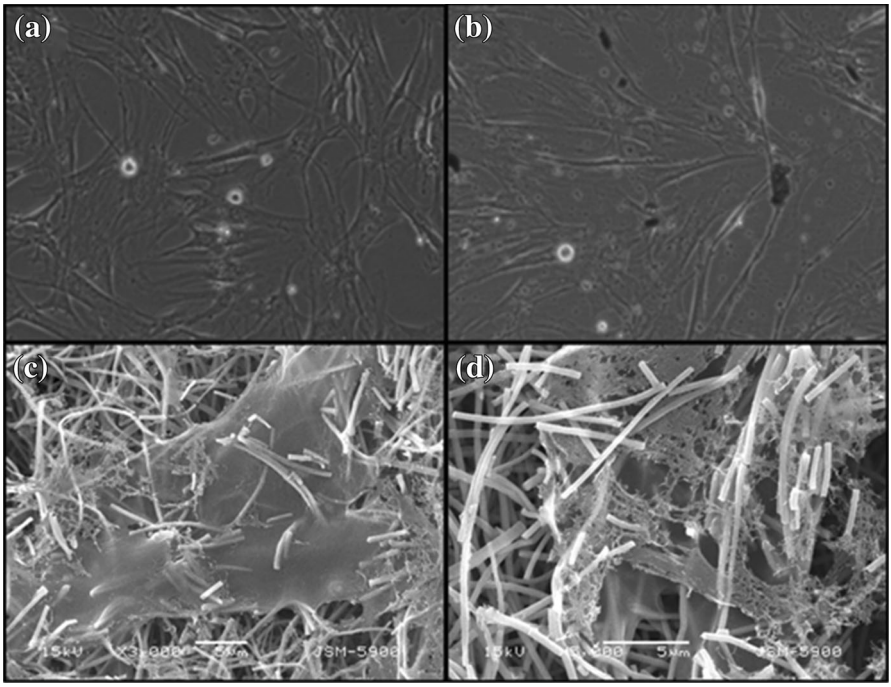

Fig. 7 Representative microscopic images of **a** unexposed control cells, **b** cells cultured in the presence of hybrid nanomatrix. Representative SEM images (**c**, **d**) of the cell fixation test on hybrid matrix

changes in adhesion assembly can alter signaling pathways which regulate cell behavior. The adhesion, motility, proliferation and differentiation behavior have been found sensitive to the nanoscale topography of matrix and has been visualized in a number of cells [30]. From the present results it has been given to understand that the synthesized hybrid nanofibers are non-toxic to the cells. The morphology of adhered cells was analyzed by SEM. Figure 7c, d shows the growth of satellite cells on Ag/TiO_2 nanofibers at the end of the incubation period. From the images, we can clearly see expansion of satellite cells on surface of hybrid nanofibers. The coarse surface (Fig. 2c) of as-synthesized nanofibers accelerated the adherence and spreading of cultured cells. Thus results obtained in the present study (Figs. 6, 7) signified that satellite cells are proliferating well on the hybrid matrix.

To acquire insight into the biological effects (specific molecular effect) of the synthesized hybrid nanofibers; microarray analysis was used to obtain functional information about the whole genomic expression profile of satellite cells (in particular, the significant genes involved in cell adhesion, proliferation, muscle development and apoptosis). The microarray technique provides information about changes of the genetic regulatory pattern of cluster of genes induced by a variety of stimuli. Considering the effectiveness of microarray technique, in the present study functional information was attained for 32,965 genes and is summarized in Tables 1 and 2. We compared the gene expression profile of satellite cells grown on the hybrid matrix with that of control cells. Out of 32,965 genes, a total of 9654 genes were up-regulated, whereas 12,325 genes were down-regulated after cultivation on nanofibers. In Fig. 8 the position of each gene on the scatter plot is determined by its expression level (cells cultured on hybrid matrix-*x*-axis and control cells-*y*-axis). Genes with identical or similar expression are depicted by a black line, whereas the gene clusters around the red line depict the $\geq$twofold up-regulation. The green solid line demonstrates the $\leq$twofold down-regulation. The red spots at the top of red line indicate $\geq$threefold up-regulation; whereas, the blue spots at the bottom of the green line illustrates $\geq$threefold down-regulation, respectively. In the present study, we identified 336 genes (1.01 % of 32,965 genes examined) whose expression level in treated cells was $\geq$twofold higher than those of control cells, and 140 genes (0.4 % of 32,965 genes examined) expression level were $\leq$twofold lower than those in control cells [31]. A total of 31 genes has been identified that were down-regulated $\leq$threefold after cultivation of satellite cells on the nanofibers. The genes have been described to participate in biological processes such as negative regulation of cell differentiation (9 genes); DNA damage (8 genes) and cellular response to stress (14 genes) have been shown in Table 1. The results suggest that cultivation of satellite cells on the hybrid nanofibers has no negative impact on the cell proliferation. Conversely, 72 genes were identified that significantly differentially up-regulated by at least $\geq$threefold after the interaction with hybrid nanomatrix. The up-regulated genes were grouped into categories according to the biological functions such as regulation of cell proliferation (32), regulation of cell activity (12), cell migration (11) and anti-apoptosis (17) (Table 2). Our observation on the basis of microarray was that the interaction of satellite cells with hybrid nanotextured matrix activates the expression of many genes mainly proliferation regulating genes (32 genes) and cell adhesion genes. In vitro culture of satellite cells on hybrid scaffold construct

Table 1 Genes significantly affected (down-regulated genes) after 48 h exposure to Ag/TiO_2 hybrid nanofibers

Functional category	Gene ID	Gene name	Species
Negative regulation of cell differentiation	NM_001046381	IQ motif containing B1	*Bos taurus*
	NM_001103255	PR domain containing 6	*Bos taurus*
	NM_001046218	SMAD family member 2	*Bos taurus*
	NM_001045877	Bone morphogenetic protein 4	*Bos taurus*
	NM_174004	Caveolin 1, caveolae protein, 22 kDa	*Bos taurus*
	NM_001046273	Cyclin D1	*Bos taurus*
	NM_203359	Dicer 1, ribonuclease type III	*Bos taurus*
	NM_001104996	Iroquois homeobox 3	*Bos taurus*
	NM_001040645	Paired box 6	*Bos taurus*
DNA damage	NM_001075790	BRCA1/BRCA2-containing complex, subunit 3	*Bos taurus*
	NM_001034433	F-box protein 6	*Bos taurus*
	NM_001024516	AlkB, alkylation repair homolog 2 (*E. coli*)	*Bos taurus*
	NM_001077874	Aprataxin and PNKP like factor	*Bos taurus*
	NM_001038530	General transcription factor IIH, polypeptide 2, 44 kDa	*Bos taurus*
	NM_001013003	Nei like 2 (*E. coli*)	*Bos taurus*
	NM_001076289	Ring finger protein 168	*Bos taurus*
	NM_174295	Structural maintenance of chromosomes 3	*Bos taurus*
Cellular response to stress	NM_001075790	BRCA1/BRCA2-containing complex, subunit 3	*Bos taurus*
	NM_001103348	ERO1-like	*Bos taurus*
	NM_001032299	ST8 alpha-*N*-acetyl-neuraminide alpha-2,8-sialyltransferase 1	*Bos taurus*
	NM_001081615	X-ray repair complementing defective repair in Chinese Hamster cells 4	*Bos taurus*
	NM_001024516	AlkB, alkylation repair homolog 2 (*E. coli*)	*Bos taurus*
	NM_001077874	Aprataxin and PNKP like factor	*Bos taurus*
	NM_001046273	Cyclin D1	*Bos taurus*
	NM_001101182	Establishment of cohesion 1 homolog 2 (*S. cerevisiae*); Similar to establishment of cohesion 1 homolog 2	*Bos taurus*
	NM_001038530	General transcription factor IIH, polypeptide 2, 44 kDa	*Bos taurus*
	NM_001013003	Nei like 2 (*E. coli*)	*Bos taurus*
	NM_001102258	Polymerase (DNA directed) kappa	*Bos taurus*
	NM_001076289	Ring finger protein 168	*Bos taurus*
	NM_001102499	Scavenger receptor class A, member 5	*Bos taurus*
	NM_174295	Structural maintenance of chromosomes 3	*Bos taurus*

Table 2 Genes significantly affected (up-regulated genes) after 48 h culture on Ag/TiO_2 hybrid nanofibers

Functional category	Gene ID	Gene name	Species
Regulation of cell proliferation	NM_001076804	GATA binding protein 3	*Bos taurus*
	NM_001101097	H2.0-like homeobox	*Bos taurus*
	NM_001025344	Nanog homeobox	*Bos taurus*
	NM_001077998	SAM and SH3 domain containing 3	*Bos taurus*
	NM_001040478	Myogenic differentiation 1	*Bos taurus*
	NM_174116	Myogenic factor 5	
	NM_173888	Adrenomedullin	*Bos taurus*
	NM_001101043	C-fos induced growth factor	*Bos taurus*
	NM_001109796	Caspase recruitment domain family, member 11	*Bos taurus*
	NM_174027	Colony stimulating factor 2 (granulocyte–macrophage)	*Bos taurus*
	NM_174298	Coxsackie virus and adenovirus receptor	*Bos taurus*
	NM_180995	Dopamine beta-hydroxylase (dopamine beta-monooxygenase)	*Bos taurus*
	NM_174043	Dopamine receptor D2	*Bos taurus*
	NM_174062	Ferritin, heavy polypeptide 1; similar to ferritin heavy chain	*Bos taurus*
	NM_178325	Growth hormone releasing hormone	*Bos taurus*
	NM_001105424	Hematopoietically expressed homeobox	*Bos taurus*
	NM_174086	Interferon, gamma	*Bos taurus*
	NM_001102175	Interleukin 20 receptor beta	*Bos taurus*
	NM_001077827	Jun oncogene	*Bos taurus*
	NM_001102478	Nerve growth factor receptor (TNFR super-family, member 16)	*Bos taurus*
	NM_001076799	Nitric oxide synthase 2, inducible	*Bos taurus*
	NM_001114515	Nuclear protein, transcriptional regulator, 1	*Bos taurus*
	NM_001075332	Parathyroid hormone 1 receptor	*Bos taurus*
	NM_173953	Prolactin	*Bos taurus*
	NM_001105323	Prostaglandin-endoperoxide synthase 1 (prostaglandin G/H synthase and cyclooxygenase)	*Bos taurus*
	NM_174445	Prostaglandin-endoperoxide synthase 2 (prostaglandin G/H synthase and cyclooxygenase)	*Bos taurus*
	NM_001130756	Retinoic acid receptor, gamma	*Bos taurus*
	NM_174176	Secretogranin II (chromogranin C)	*Bos taurus*
	NM_001034333	Spermidine/spermine N1-acetyltransferase 1	*Bos taurus*
	NM_001075912	Stratifin	*Bos taurus*
	NM_173966	Tumor necrosis factor (TNF super-family, member 2)	*Bos taurus*
	NM_001098980	V-maf musculoaponeurotic fibrosarcoma oncogene homolog G	*Bos taurus*

Table 2 continued

Functional category	Gene ID	Gene name	Species
Regulation of cell activity	NM_001103225	CD4 molecule	*Bos taurus*
	NM_001034735	CD74 molecule, major histocompatibility complex, class II invariant chain	*Bos taurus*
	NM_001077998	SAM and SH3 domain containing 3	*Bos taurus*
	NM_173895	Bactericidal/permeability-increasing protein	*Bos taurus*
	NM_174297	Cytotoxic T-lymphocyte-associated protein 4	*Bos taurus*
	NM_001038674	Lipopolysaccharide binding protein	*Bos taurus*
	NM_001034334	Lymphocyte-specific protein tyrosine kinase	*Bos taurus*
	NM_174198	Toll-like receptor 4	*Bos taurus*
	NM_001101855	Tumor necrosis factor (ligand) super-family, member 14	*Bos taurus*
	NM_174087	Insulin-like growth factor 2 (somatomedin A)	*Bos taurus*
	NM_174093	Interleukin 1, beta	*Bos taurus*
	NM_173950	Placental growth factor	*Bos taurus*
Cell migration	NM_001046569	Chemokine (C–C motif) ligand 25	*Bos taurus*
	NM_001046603	Cholecystokinin	*Bos taurus*
	NM_174512	Cyclin-dependent kinase 5, regulatory subunit 1 (p35)	*Bos taurus*
	NM_174309	Endothelin receptor type B	*Bos taurus*
	NM_174348	Intercellular adhesion molecule 1	*Bos taurus*
	NM_173925	Interleukin 8	*Bos taurus*
	NM_001110000	Kinase insert domain receptor (a type III receptor tyrosine kinase)	*Bos taurus*
	NM_181037	Nitric oxide synthase 3 (endothelial cell)	*Bos taurus*
	NM_174181	Selectin E	*Bos taurus*
	NM_174183	Selectin P	*Bos taurus*
	NM_001101045	Zinc finger, AN1-type domain 5	*Bos taurus*
Anti-apoptosis	NM_001082471	BCL2-associated athanogene 3	*Bos taurus*
	NM_173896	Betacellulin	*Bos taurus*
	NM_174290	Crystallin, alpha B	*Bos taurus*
	NM_174067	Ghrelin/obestatin prepropeptide	*Bos taurus*
	NM_001083674	Glutamate-cysteine ligase, catalytic subunit	*Bos taurus*
	NM_203322	Heat shock 70 kDa protein 1A	*Bos taurus*
	NM_174121	Neurofilament, light polypeptide	*Bos taurus*
	NM_181037	Nitric oxide synthase 3 (endothelial cell)	*Bos taurus*
	NM_001166512	Protein C (inactivator of coagulation factors Va and VIIIa)	*Bos taurus*
	NM_001031750	Forkhead box L2	*Bos taurus*
	NM_001075647	Myosin light chain, phosphorylatable, fast skeletal muscle	*Bos taurus*
	NM_174225	Nucleoporin 133 kDa; actin, alpha 1, skeletal muscle	*Bos taurus*

Table 2 continued

Functional category	Gene ID	Gene name	Species
	NM_001082471	BCL2-associated athanogene 3	*Bos taurus*
	NM_174290	Crystallin, alpha B	*Bos taurus*
	NM_001083674	Glutamate-cysteine ligase, catalytic subunit	*Bos taurus*
	NM_203322	Heat shock 70 kDa protein 1A	*Bos taurus*
	NM_181037	Nitric oxide synthase 3 (endothelial cell)	*Bos taurus*
Cell adhesion	*NM_001001601*	Cadherin 5, type 2 (vascular endothelium)	*Bos taurus*
	NM_001076460	Claudin 5	*Bos taurus*
	NM_001078066	Endothelial cell adhesion molecule	*Bos taurus*
	NM_174348	Intercellular adhesion molecule 1	*Bos taurus*
	NM_174571	Platelet/endothelial cell adhesion molecule	*Bos taurus*
	NM_174181	Selectin E	*Bos taurus*
	NM_174183	Selectin P	*Bos taurus*
	NM_001101158	Vascular cell adhesion molecule 1	*Bos taurus*
Muscle organ development	NM_001101097	H2.0-like homeobox	*Bos taurus*
	NM_174290	Crystallin, alpha B	*Bos taurus*
	NM_001031750	Forkhead box L2	*Bos taurus*
	NM_001075647	Myosin light chain, phosphorylatable, fast skeletal muscle	*Bos taurus*
	NM_001035025	Myosin, light chain 2, regulatory, cardiac, slow	*Bos taurus*
	NM_174225	Nucleoporin 133 kDa; actin, alpha 1, skeletal muscle	*Bos taurus*
	NM_001081721	Transcription factor 15 (basic helix–loop-helix)	*Bos taurus*
	NM_001038216	Transcription factor 23	*Bos taurus*
	NM_001101045	Zinc finger, AN1-type domain 5	*Bos taurus*

and sequential expression of a cluster of genes after biological interaction are schematically illustrated in Fig. 9. From the in vitro tests and microarray analysis, it was concluded that Ag/TiO_2 hybrid matrix showed a beneficial effect on the adhesion and growth of muscle satellite cells, therefore suggest them to be used in biomedical applications especially muscle tissue engineering.

In summary, Ag/TiO_2 crossbreed nanofibrous matrix with increased surface area was prepared via cost-effective e-spinning method. We isolated the satellite cells from adult Hanwoo muscle and the isolated muscle precursor cells were for the first time cultivated on the electrospun Ag/TiO_2 hybrid nanofibers under in vitro conditions. A total of 31 genes has been identified that were down-regulated ($\leq$threefold) after interaction of satellite cells with nanofibers. The genes have been described to participate in cellular response to stress, negative regulation of cell differentiation and DNA damage. It is given to understand that the cultivation of satellite cells on the hybrid nanofibers has no negative impact on the cell proliferation. Conversely, 72 genes were identified to be significantly up-regulated ($\geq$threefold) after the interaction with hybrid nanomatrix. The up-regulated genes

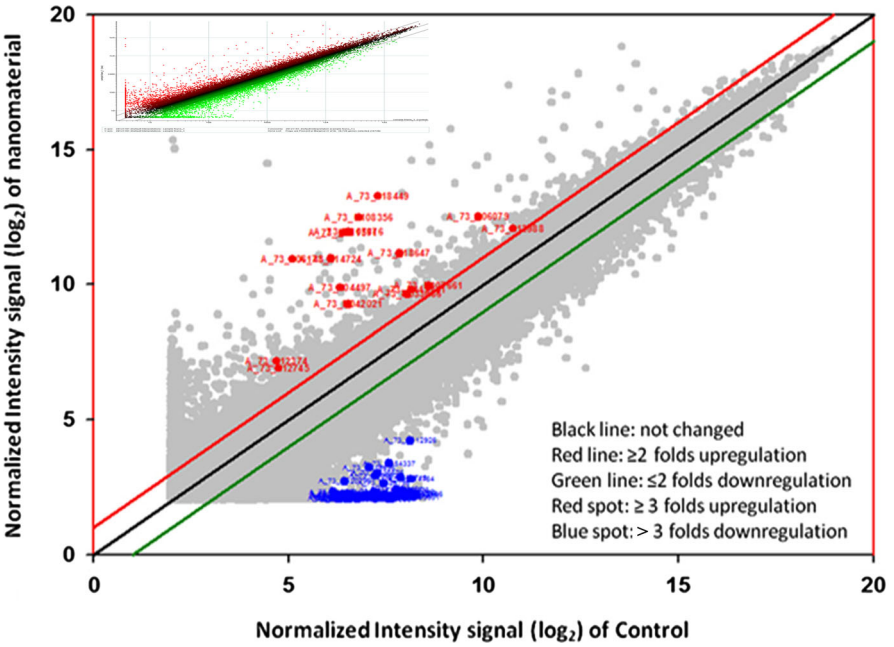

Fig. 8 Gene expression profile of satellite cells cultivated on nanomatrix. The global gene expression profiles of control or treated cells were assessed using oligonucleotide microarray analysis. A total of 32,965 genes present on the bovine gene expression microarray were plotted using a scatter plot. The position of each gene on the plot is determined by its expression levels in control (*x* axis) and satellite cells on nanomatrix (*y* axis)

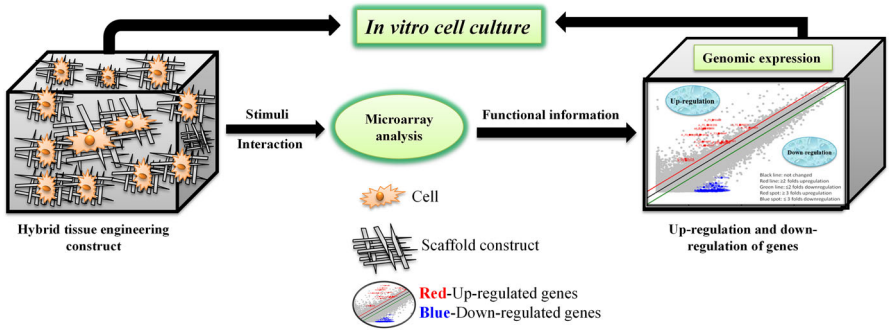

Fig. 9 Schematic illustration of in vitro culture of satellite cells on hybrid scaffold construct and sequential expression of a cluster of genes after a biological interaction

participate in the biological functions such as regulation of cell proliferation, regulation of cell activity, cell migration and anti-apoptosis. In a recent report, the reference gene stability in peripheral blood mononuclear cells was determined by qPCR and NanoString [32]. In the present investigation, we have used the microarray technique. Nowadays the microarray DNA hybridization techniques

have been used widely from basic to applied molecular biology research to study which genes are active and which are inactive in different cell types. This helps to understand both how these cells function normally and how they are affected when various genes do not perform properly. With the development of DNA microarray technology, however, now we can examine how active thousands of genes are at any given time phase. Microarray technology helped researchers to learn more about various different diseases (heart disease, mental illness and infectious diseases, etc.). From the earlier studies it has been given to understand that TiO_2 nanotubes result in accelerated cell adhesion and growth with faster propagation of filopodia [33]. Moreover, the highest cell activity such as cell attachment and proliferation was observed on the TiO_2 nanotubes [13]. Previous existing literature clearly indicates the efficacy of TiO_2 nanotube structures in eliciting cellular response in terms of adhesion, proliferation and differentiation by varying various parameters such as tube diameter, crystallinity and length [34]. Therefore, titania nanofibers/nanotubes and their composites are attracting immense recognition as an implantation material due to their exceptional qualities such as high specific surface area and the ability to exhibit positive cellular response. Most recently Peng et al. also reported that TiO_2 nanotubes enhance osteogenic gene expression and differentiation in osteoblasts cells [35]. However, to the best of our knowledge the information about the effects of Ag/TiO_2 hybrid nanofibers on whole-genome mRNA expression of muscle satellite cells derived from Korean native cattle Hanwoo is still lacking. The present study was the first in which microarray technique was employed to detect possible Ag/TiO_2 hybrid matrix-specific effects. The coarse surface of as-synthesized nanofibers accelerated the proliferation and also expressed up-regulation of proliferation, cell adhesion and muscle differentiation/development genes.

Conclusions

In summary, we isolated the satellite cells from adult Hanwoo muscle and the isolated muscle precursor cells were for the first time were cultivated on Ag/TiO_2 hybrid nanofibers under in vitro conditions. Ag/TiO_2 nanofibrous matrix with increased surface area was prepared via cost-effective electrospinning method. Microarray technique was employed to detect potential matrix-specific effects. Results from this study first time provide insights into the molecular mechanisms of the response of muscle precursor cells to Ag/TiO_2 hybrid matrix. Our observation on the basis of microarray analysis was that the interaction of satellite cells with hybrid nanotextured matrix activates the expression of many genes mainly proliferation regulating and adhesion genes. This paves the way for development and analysis of gene expression biomarkers for native Korean Hanwoo satellite cell proliferation and as a final point to muscle tissue engineering. Thus, the results of present study provide constructive information regarding the muscle tissue engineering.

Acknowledgments This work has been supported by a grant from Next Generation Bio-green 21 (No. PJ01110102) and Rural Development Administration (RDA)-Free Trade Agreement (FTA) strategy issues (No. PJ01017003). The authors also extend their appreciation to the Deanship of Scientific Research (RGP-VPP-089) at King Saud University for the help in research work.

References

1. Taylor P, Ussher A, Burrell R (2005) Impact of heat on nanocrystalline silver dressings: part I: chemical and biological properties. Biomaterials 26:7221–7229
2. Kim J, Cho M, Oh B, Choi S, Yoon J (2004) Control of bacterial growth in water using synthesized inorganic disinfectant. Chemosphere 55:775–780
3. Berger T, Spadaro J, Bierman R, Chapin S, Becker R (1976) Antifungal properties of electrically generated metallic ions. Antimicrob Agents Chemother 10:856–860
4. Kusnetsov J, Iivanainen E, Elomaa N, Zacheus O, Martikainen PJ (2001) Copper and silver ions more effective against legionellae than against mycobacteria in a hospital warm water system. Water Res 35:4217–4225
5. Russell AD, Hugo WB (1994) Antimicrobial activity and action of silver. Prog Med Chem 31:351–370
6. Arora S, Jain J, Rajwade J, Paknikar K (2009) Interactions of silver nanoparticles with primary mouse fibroblasts and liver cells. Toxicol Appl Pharmacol 236:310–318
7. Tolaymat TM, El Badawy AM, Genaidy A, Scheckel KG, Luxton TP, Suidan M (2010) An evidence-based environmental perspective of manufactured silver nanoparticle in syntheses and applications: a systematic review and critical appraisal of peer-reviewed scientific papers. Sci Total Environ 408:999–1006
8. Ahamed M, AlSalhi MS, Siddiqui M (2010) Silver nanoparticle applications and human health. Clin Chim Acta 411:1841–1848
9. Kim S, Choi JE, Choi J, Chung K-H, Park K, Yi J et al (2009) Oxidative stress-dependent toxicity of silver nanoparticles in human hepatoma cells. Toxicol In Vitro 23:1076–1084
10. Kim JS, Kuk E, Yu KN, Kim J-H, Park SJ, Lee HJ et al (2007) Antimicrobial effects of silver nanoparticles. Nanomed Nanotechnol Biol Med 3:95–101
11. Hernández-Sierra JF, Ruiz F, Cruz Pena DC, Martínez-Gutiérrez F, Martínez AE, de Jesús Pozos Guillén A et al (2008) The antimicrobial sensitivity of *Streptococcus mutans* to nanoparticles of silver, zinc oxide, and gold. Nanomed Nanotechnol Biol Med 4:237–240
12. Oh S, Brammer KS, Li YJ, Teng D, Engler AJ, Chien S et al (2009) Stem cell fate dictated solely by altered nanotube dimension. Proc Natl Acad Sci 106:2130–2135
13. Brammer KS, Oh S, Cobb CJ, Bjursten LM (2009) Heyde Hvd, Jin S. Improved bone-forming functionality on diameter-controlled TiO_2 nanotube surface. Acta Biomater 5:3215–3223
14. Liu S, Chen A (2005) Coadsorption of horseradish peroxidase with thionine on TiO_2 nanotubes for biosensing. Langmuir 21:8409–8413
15. Bigerelle M, Anselme K, Noel B, Ruderman I, Hardouin P, Iost A (2002) Improvement in the morphology of Ti-based surfaces: a new process to increase in vitro human osteoblast response. Biomaterials 23:1563–1577
16. Brammer KS, Oh S, Gallagher JO, Jin S (2008) Enhanced cellular mobility guided by TiO_2 nanotube surfaces. Nano Lett 8:786–793
17. Yu W, Zhang Y, Jiang X, Zhang F (2010) In vitro behavior of MC3T3-E1 preosteoblast with different annealing temperature titania nanotubes. Oral Dis 16:624–630
18. Smith BS, Yoriya S, Johnson T, Popat KC (2011) Dermal fibroblast and epidermal keratinocyte functionality on titania nanotube arrays. Acta Biomater 7:2686–2696
19. Burns K, Yao C, Webster TJ (2009) Increased chondrocyte adhesion on nanotubular anodized titanium. J Biomed Mater Res Part A 88:561–568
20. Peng L, Eltgroth ML, LaTempa TJ, Grimes CA, Desai TA (2009) The effect of TiO_2 nanotubes on endothelial function and smooth muscle proliferation. Biomaterials 30:1268–1272
21. Park J, Bauer S, von der Mark K, Schmuki P (2007) Nanosize and vitality: TiO_2 nanotube diameter directs cell fate. Nano Lett 7:1686–1691
22. Bauer S, Park J, Faltenbacher J, Berger S, von der Mark K, Schmuki P (2009) Size selective behavior of mesenchymal stem cells on ZrO_2 and TiO_2 nanotube arrays. Integr Biol. 1:525–532

23. Sun B, Long Y, Zhang H, Li M, Duvail J, Jiang X et al (2014) Advances in three-dimensional nanofibrous macrostructures via electrospinning. Prog Polym Sci 39:862–890
24. Popat KC, Leoni L, Grimes CA, Desai TA (2007) Influence of engineered titania nanotubular surfaces on bone cells. Biomaterials 28:3188–3197
25. Ainslie KM, Tao SL, Popat KC, Daniels H, Hardev V, Grimes CA et al (2009) In vitro inflammatory response of nanostructured titania, silicon oxide, and polycaprolactone. J Biomed Mater Res Part A 91:647–655
26. Amna T, Hassan MS, Van Ba H, Khil M-S, Lee H-K, Hwang IH (2013) Electrospun Fe_3O_4/TiO_2 hybrid nanofibers and their in vitro biocompatibility: prospective matrix for satellite cell adhesion and cultivation. Mater Sci Eng C 33:707–713
27. Amna T, Hassan MS, Shin WS, Van Ba H, Lee HK, Khil MS et al (2013) TiO_2 nanorods via one-step electrospinning technique: a novel nanomatrix for mouse myoblasts adhesion and propagation. Colloids Surf B 101:424–429
28. Siva Vijayakumar T, Karthikeyeni S, Vasanth S, Ganesh A, Bupesh G, Ramesh R, et al (2013) Synthesis of silver-doped zinc oxide nanocomposite by pulse mode ultrasonication and its characterization studies. J Nanosci 2013:1–7
29. Chen S-S, Hsi H-C, Nian S-H, Chiu C-H (2014) Synthesis of N-doped TiO_2 photocatalyst for low-concentration elemental mercury removal under various gas conditions. Appl Catal B 160:558–565
30. Amna T, Shamshi Hassan M, Khil MS, Lee HK, Hwang I (2014) Electrospun nanofibers of ZnO–TiO_2 hybrid: characterization and potential as an extracellular scaffold for supporting myoblasts. Surf Interface Anal 46:72–76
31. Kaveh R, Li YS, Ranjbar S, Tehrani R, Brueck CL, Van Aken B (2013) Changes in *Arabidopsis thaliana* gene expression in response to silver nanoparticles and silver ions. Environ Sci Technol 47:10637–10644
32. Radke L, Giese C, Lubitz A, Hinderlich S, Sandig G, Hummel M, et al (2014) Reference gene stability in peripheral blood mononuclear cells determined by qPCR and NanoString. Microchim Acta 181(13):1733–1742
33. Oh S, Daraio C, Chen LH, Pisanic TR, Finones RR, Jin S (2006) Significantly accelerated osteoblast cell growth on aligned TiO_2 nanotubes. J Biomed Mater Res Part A 78:97–103
34. Tan A, Pingguan-Murphy B, Ahmad R, Akbar S (2012) Review of titania nanotubes: fabrication and cellular response. Ceram Int 38:4421–4435
35. Peng J, Zhang X, Li Z, Liu Y, Yang X (2015) Titania nanotube delivery fetal bovine serum for enhancing MC3T3-E1 activity and osteogenic gene expression. Mater Sci Eng C 56:438–443